

Supporting Information

A Nanophase-separated, Quasi-solid State Polymeric Single Ion Conductor: Polysulfide Exclusion for Lithium Sulfur Batteries

Jinhong Lee^a, Jongchan Song^a, Hongkyung Lee^b, Hyungjun Noh^a, Yun-Jung Kim^a, Sung Hyun Kwon^c, Seung Geol Lee^c, Hee-Tak Kim^{a}*

^aJ. Lee, Dr. J. Song, Dr. H. Lee, H. Noh, Y. Kim, Prof. H.-T. Kim
Department of Chemical and Biomolecular Engineering, Korea Advanced Institute of Science and Technology, Daejeon 305-701, South Korea

^bH.Lee

Energy and Environment Directorate Pacific Northwest National Laboratory 902 Battelle Boulevard, Richland, WA 99354, USA

^cS. H. Kwon, Prof. S. G. Lee

Department of Organic Material Science and Engineering, Pusan National University, Busandaehak-ro 63 beon-gil, Geumjeong-gu, Busan 46241, South Korea

Corresponding Author

*Email: heetak.kim@kaist.ac.kr

METHODS/EXPERIMENTAL

Lithiation of the PFSA membrane and ionomer. A PFSA membrane in a protonated form was purchased, and its lithiation was carried out in a solution of 2.0 M LiOH in a H₂O: EtOH (2:1 by weight) mixture at 80°C for 6 h under vigorous stirring. The resulting lithiated membrane was rinsed in deionized water to remove any residual salt.²² Additionally, a protonated PFSA ionomer dispersed in an isopropyl alcohol/water mixture was lithiated in the same manner for use in the SPSIC-based sulfur cathode.

Fabrication of the sulfur cathodes. A sulfur/carbon (Ketjen black) composite (S/C=60/40 in weight) was prepared with the melt diffusion method. A slurry consisting of the S/C composite (20 wt%), vapor grown carbon fiber (10 wt%), and Li-PFSA (70 wt%) was cast onto an etched Al foil. The cast was dried at 60°C for 24 h, and then, the resulting sulfur cathode was compressed by a roll press to congregate the cathode ingredients until the cathode thickness was reduced by 30% (cathode thickness: 20 μm). The sulfur loading was controlled at 0.2 mg cm⁻².

Measurement of solvent uptake and ionic conductivity. The solvent uptake of SPSIC, which is the percent weight ratio between the solvent and Li-PFSA polymer, was determined by measuring the weight gain after fully equilibrating the Li-PFSA membrane in salt-free solvents. The ionic conductivity of the SPSIC was determined from the EIS data for the corresponding SUS/SPSIC/SUS symmetric cells.

Electrochemical Measurements. Cell assembly was conducted in an Ar-filled glove box. The SPSIC-based Li-S cells were fabricated by staking the Li metal (Honjo Metal, 450 μm), SPSIC membrane (16 μm), and sulfur cathode in a 2032 type coin cell and clamping the cell. The liquid electrolyte-containing Li-S batteries were also fabricated with a 20 μm thick porous PP separator and 1 M lithium bis(trifluoromethanesulfonyl)imide (LiTFSI) S50/D50

electrolyte. These cells were cycled between 1.6 and 2.8 V at a constant current (0.1 C, 167.5 mA_{g-sulfur-1}) and at room temperature with a battery cycler (Won-A-tech). EIS was measured in the frequency range of 0.1 Hz to 1 MHz with a frequency response analyzer (Solatron 1255).

Material Characterization. The surface and cross section morphologies of the sulfur cathodes were observed by FE-SEM (Sirion, FEI). The PS concentration in the SPSIC was measured with a UV spectrophotometer (V-570, Jasco). The solvent cluster size of the SPSIC was determined with a small angle X-ray scattering apparatus (RIGAKU, D/MAX-2500).

Table S1. The comparisons between the previous research and our current work.

	Material used	Configuration in the cell	Key physicochemical concept
The current work	Lithiated Nafion swollen with <u>Li salt-free sulfolane/diglyme mixture</u>	<u>Whole electrolyte medium</u>	<u>Thermodynamic PS exclusion</u>
ChemSusChem 2014, 7, 3341 ¹	Lithiated Nafion swollen with 1M LiTFSI in DOL /DME (v/v = 1/1)	Thin layer on the cathode	Kinetic barrier for PS dissolution into bulk electrolyte phase
J. Mater. Chem. A 2015, 3, 323 ²	Poly (α -lipoic acid) swollen with 1M LiTFSI in DOL /DME (v/v = 1/1)	Thin layer on the cathode	Kinetic barrier for PS dissolution into bulk electrolyte phase
J. PowerSources 2014, 4, 251, 417 ³	Lithiated Nafion swollen with 1M LiTFSI in DOL /DME (v/v = 1/1)	Separator	Kinetic barrier for PS diffusion toward Li metal. Electrostatic repulsion between PS and Nafion
Chem. Mater. 2016, 28, 5147 ⁴	Cross-linked polyethylene glycol (PEG) framework containing pendant SO ₃ ⁻ group swollen with 1M LiTFSI in DOL /DME (v/v = 1/1)	Separator	Kinetic barrier for PS diffusion toward Li metal. Electrostatic repulsion between PS and Nafion

Supplementary Note 1

Donnan exclusion effect

It is considered a lithium polysulfide (PS)-containing liquid electrolyte phase and a lithiated perfluorinated sulfonic acid (Li-PFSA) phase in contact. When the two phases are equilibrated, the Li-PFSA swells the liquid electrolyte, and the Li^+ , TFSI^- , and S_n^{2-} ions are distributed in the two phases schematically illustrated in Fig. S. 1. C_{Li^+} , C_{TFSI^-} , and $C_{\text{S}_n^{2-}}$ are the concentrations of the Li^+ , TFSI^- , and S_n^{2-} in the electrolyte phase, respectively. The concentrations of the Li^+ , TFSI^- , and SO_3^- of the Li-PFSA and S_n^{2-} in the electrolyte-swollen Li-PFSA phase are denoted as \bar{C}_{Li^+} , \bar{C}_{TFSI^-} , $\bar{C}_{\text{SO}_3^-}$, $\bar{C}_{\text{S}_n^{2-}}$, respectively.

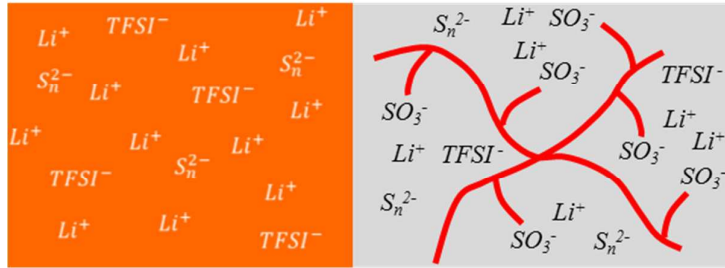


Figure S1.1. Schematic illustration of the PS-containing liquid electrolyte and the electrolyte-swollen Li-PFSA in equilibrium.

From electroneutrality considerations, for the electrolyte phase,

$$C_{\text{Li}^+} = C_{\text{TFSI}^-} + 2C_{\text{S}_n^{2-}} \quad (1)$$

and in the Li-PFSA phase,

$$\bar{C}_{\text{Li}^+} = \bar{C}_{\text{TFSI}^-} + \bar{C}_{\text{SO}_3^-} + 2\bar{C}_{\text{S}_n^{2-}} \quad (2)$$

At equilibrium, the electrochemical potential of each ion in the two phases is equal. For simplicity, the activity coefficient is assumed to be unity in further derivations. For the Li ion,

the electrochemical potential can be expressed as follows in equation (3):

$$\mu_{Li^+}^{\circ} + RT \ln C_{Li^+} + F\Psi = \mu_{Li^+}^{\circ} + RT \ln \bar{C}_{Li^+} + F\bar{\Psi}, \quad (3)$$

where μ , Ψ , and F denote the chemical potential, electrical potential (Donnan potential), and Faraday's constant, respectively. Similar relationships can be written for the TSFI and PS anions given in equations (4) and (5).

$$\mu_{TFSI^-}^{\circ} + RT \ln C_{TFSI^-} - F\Psi = \mu_{TFSI^-}^{\circ} + RT \ln \bar{C}_{TFSI^-} - F\bar{\Psi} \quad (4)$$

$$\mu_{S_n^{2-}}^{\circ} + RT \ln C_{S_n^{2-}} - 2F\Psi = \mu_{S_n^{2-}}^{\circ} + RT \ln \bar{C}_{S_n^{2-}} - 2F\bar{\Psi} \quad (5)$$

By combining equations (3), (4), and (5), the difference in electric potential can be expressed in terms of the concentration ratios of the two phases shown in equation (6).

$$\frac{F(\Psi - \bar{\Psi})}{RT} = \ln \frac{C_{Li^+}}{\bar{C}_{Li^+}} = \ln \frac{\bar{C}_{TFSI^-}}{C_{TFSI^-}} = \ln \left(\frac{\bar{C}_{S_n^{2-}}}{C_{S_n^{2-}}} \right)^{1/2} \quad (6)$$

From equation (6),

$$C_{Li^+} C_{TFSI^-} = \bar{C}_{Li^+} \bar{C}_{TFSI^-} \quad (7)$$

$$C_{Li^+}^2 C_{S_n^{2-}} = \bar{C}_{Li^+}^2 \bar{C}_{S_n^{2-}} \quad (8)$$

By combining equations (2), (7), and (8), an analytical expression for the PS concentration ratio between the electrolyte phase and the swollen Li-PFSA phase can be obtained as equation (9).

$$x^3 + \frac{C_{TFSI^-}}{2C_{S_n^{2-}}} x^2 + \frac{\bar{C}_{SO_3^-}}{2C_{S_n^{2-}}} x - \frac{C_{Li^+}}{2C_{S_n^{2-}}} = 0, \quad x = \sqrt{\frac{\bar{C}_{S_n^{2-}}}{C_{S_n^{2-}}}} \quad (9)$$

Equation (9) can be numerically solved with a Newton-Raphson procedure. According to

equation (9), the dependences of $\bar{C}_{S_n^{2-}}/C_{S_n^{2-}}$ on $C_{TFSI^-}/C_{S_n^{2-}}$ and $\bar{C}_{SO_3^-}/C_{S_n^{2-}}$ are shown in Figure S1.2. The PS concentration in the Li-PFSA phase decreases with the increase in the SO_3^- concentration in the Li-PFSA phase and with the decrease in the TFSI concentration. Therefore, a higher PS rejection is expected with a lower LiTFSI salt concentration in the bulk electrolyte.

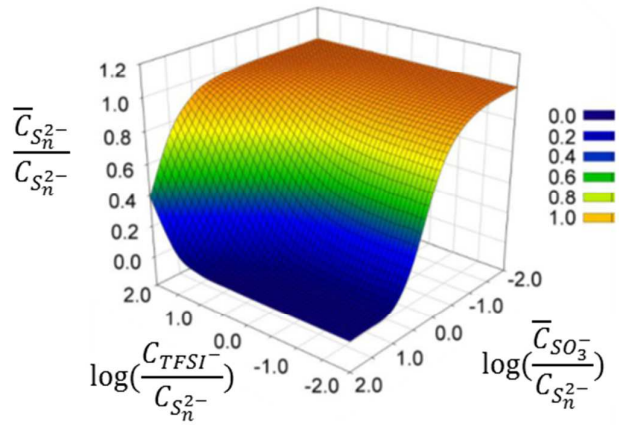


Figure S1.2. 3-dimensional plot of $\bar{C}_{S_n^{2-}}/C_{S_n^{2-}}$ as function of $C_{TFSI^-}/C_{S_n^{2-}}$ and $\bar{C}_{SO_3^-}/C_{S_n^{2-}}$ according to equation (9)

Supplementary Note 2

Small-angle X-ray scattering (SAXS) analysis

If it is assumed that the clusters of Li-PFSA polymer are approximately spherical, the cluster diameter can be calculated from the amount of solvent absorption and SAXS data. The volume change during the swelling of the Li-PFSA polymer with organic solvent can be calculated by equation (10):

$$\Delta V = \frac{\rho_p \Delta m}{\rho_s} \quad (10)$$

where, ΔV is the fractional volume change (volume difference between the swollen polymer and dry polymer); Δm is the fractional weight gain; ρ_p and ρ_s are the density of the dry polymer and salt free solvent, respectively. The volume of the cubic lattice (V_c) can be calculated with the bragg spacing ($d = \frac{\lambda}{2 \sin \theta}$) observed in the SAXS data.

$$V_c = \left[\frac{\Delta V}{1 + \Delta V} \right] d^3 + N_p V_p \quad (11)$$

N_p is the number of ion-exchange sites in a cluster, and $V_p (6.8 \times 10^{-23})$ is the volume of an exchange site. N_p can be obtained from the density and equivalent weight $M_{eq}(1000)$ of the Li-PFSA from equation (12):

$$N_p = \left[\frac{N_A \rho_p \Delta m}{18(1 + \Delta V)} \right] d^3 \quad (12)$$

, where N_A is Avogadro's number. From the value of V_c , the cluster diameter d_c can be obtained with equation (13).

$$d_c = \sqrt[3]{\frac{6V_c}{\pi}} \quad (13)$$

The various parameters used in the calculation of d_c are listed for the SPSICs with different solfolane/digyme ratios in Table S1.

Table S2. List of the parameters used for the calculation of d_c and the resulting values for d_c

SPSIC	Solvent density (ρ_s, g/cm³)	Mass gain (100Δm, %)	Volume gain (100ΔV, %)	Bragg spacing (d, nm)	Cluster diameter (d_c, nm)
0S/100D	0.937	20.1	42.1	3.37	2.95
20S/80D	1.00	32.2	67.3	3.94	3.74
50S/50D	1.09	59.6	126	5.74	5.98
80S/20D	1.20	69.2	145	6.14	6.51

Table S3. Ionic conductivities and solvent uptake of the SPSICs prepared with various solvents at room temperature.

Solvent	Li ⁺ conductivity ($\times 10^{-5} \text{ S cm}^{-1}$)	Solvent uptake (%)
EC/PC (1/1)	15.0	90.6
Sulfolane	5.01	71.3
S80/D20	3.88	69.2
S50/D50	2.60	59.6
S20/D80	1.05	32.2
Diglyme (S0/D100)	0.595	20.1
TEGDME	0.402	30.4
Dimethyl ether	0.175	14.0
Dioxolane	0.0665	9.04

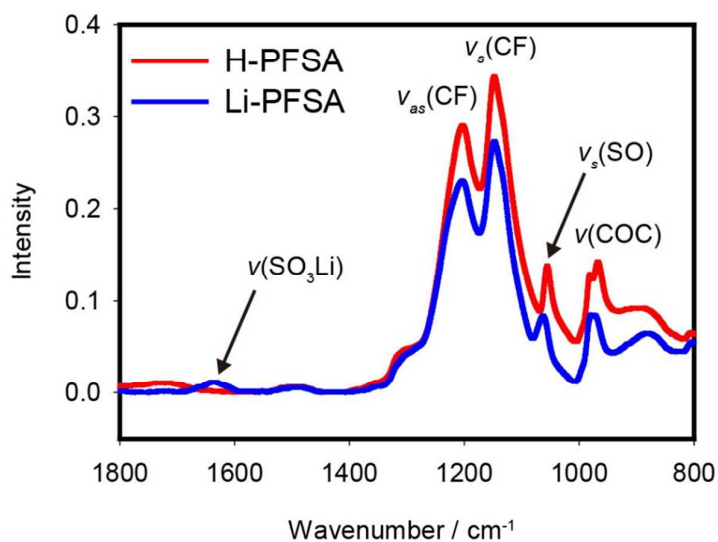


Figure S2. FT-IR spectra of the pristine PFSA and lithiated PFSA membrane.

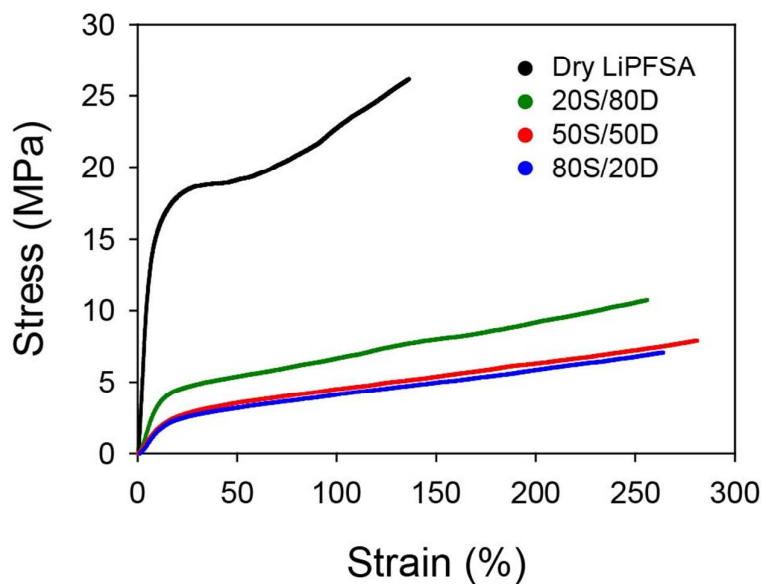


Figure S3. Strain-stress curves for the dry Li-PFSA polymer and the SPSIC-20S/80D, -50S/50D, and -80S/20D

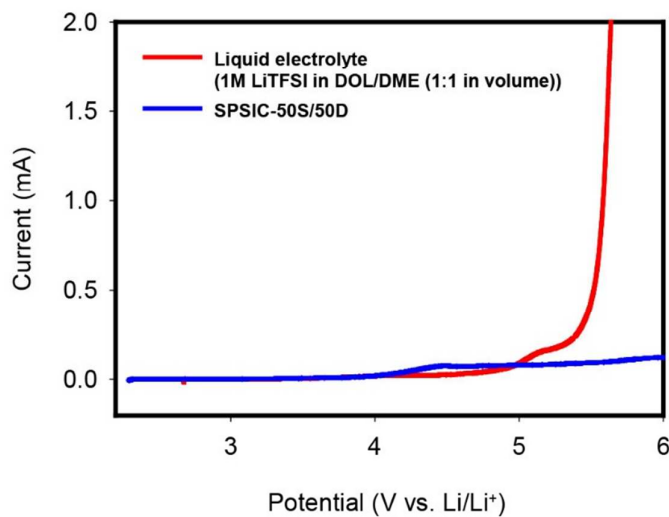


Figure S4. Linear sweep voltammetry curves for the SPSIC-50S/50D and a liquid electrolyte (1M LiTFSI in DOL/DME (1:1 in volume)) measured at a scan rate of 2 mV sec⁻¹.

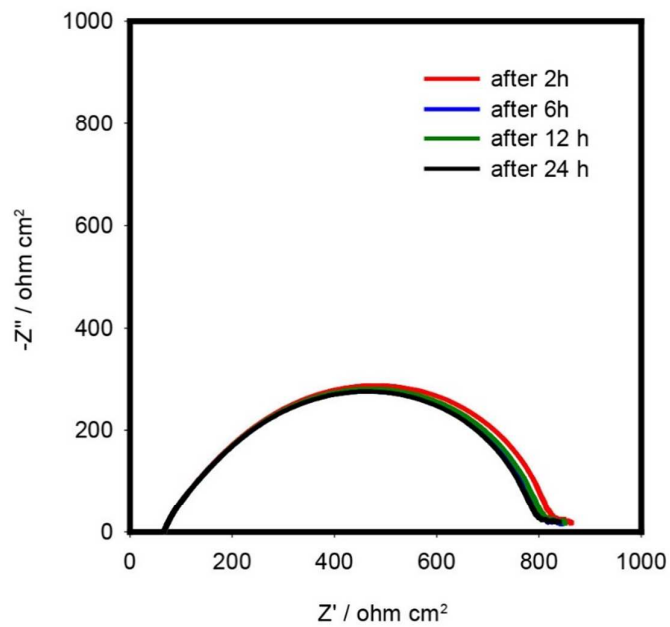


Figure S5. Nyquist plots of the impedances of a Li-Li symmetric cell with SPSIC-50S/50D membrane measured at storage times of 2, 6, 12, and 24 h.

Supplementary Note 3

Molecular dynamics simulation

All simulations were done with a fully atomistic model of the PFSA membrane (Figure S1.1), sulfolane, diglyme and Li ion. We constructed models with 32 PFSA polymer chains, 912 sulfolane molecules, 608 diglyme molecules and 320 Li ions using Monte Carlo methods to obtain the most stable initial model (The total number of atoms in this model is 46928.). The model is built for the SPSIC-50S/50D system.

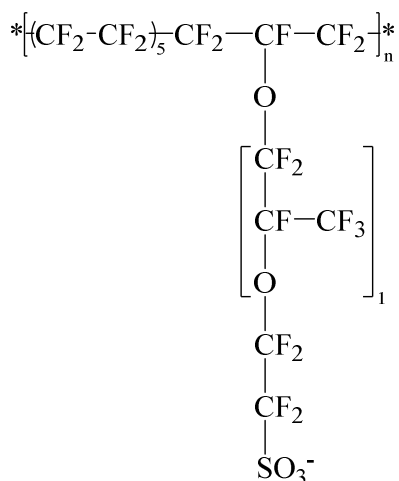


Figure S6-1. The chemical structure of the PFSA membrane.

We applied an annealing procedure for the relaxation of the system for any possible significant local minima. This approach has been successfully used on polymeric systems.⁵⁻⁸ Following the annealing procedure, a subsequent 20 ns NPT molecular dynamics (MD) simulation was performed to obtain the equilibrated system. Data collection for the pair correlation function analysis was obtained by performing another 5 ns NPT MD simulation. The energy profiles and volume profile for the last 5 ns NPT MD simulation are shown in

Figure S3-1. Based on the profiles, we confirmed that the model system is equilibrated.

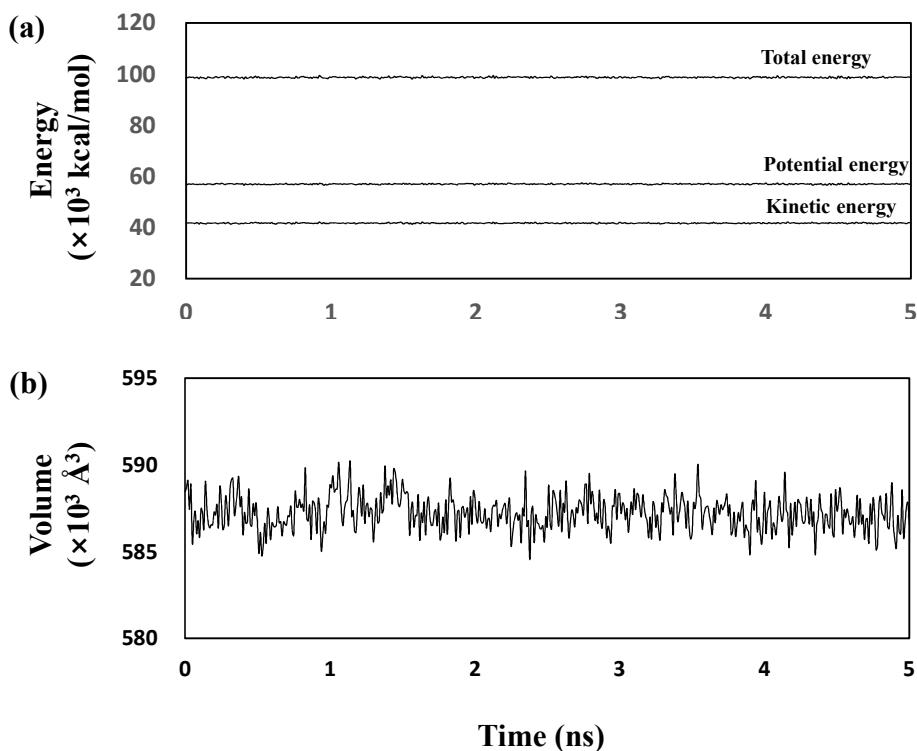


Figure S6-2. (a) Energy profile and (b) volume profile of the last 5 ns NPT MD simulation.

We used the modified DREIDING force field⁹ for this investigation. The DREIDING force field has been successfully used for various organic based systems including polymer electrolyte membranes.^{5,6, 10-13} For the Li ion, we used the OPLS based force field which is specifically designed for ionic liquid simulations.¹⁴ The total force field can be written as follows:

$$E_{total} = E_Q + E_{vdW} + E_{bond} + E_{angle} + E_{torsion} + E_{inversion} \quad (1)$$

, where E_{total} , E_Q , E_{vdW} , E_{bond} , E_{angle} , $E_{torsion}$, and $E_{inversion}$ are the energies for the total,

electrostatic, van der Waals, bond stretching, angle bending, torsion and inversion energy, respectively. For the MD simulations, the velocity-Verlet algorithm method was used to integrate the equations of motion with a time step of 1.0 fs. A Nose-Hoover thermostat and Andersen-Hoover barostat were used for this investigation. The atomic charges were assigned with the Mulliken population analysis¹⁵ at the level of the GGA-PBE functional with the DNP basis set. The Particle-Particle Particle-Mesh (PPPM) method was used to calculate the electrostatic interactions. The MD simulation code used in this study was the Large-scale Atomic/Molecular Massively Parallel Simulator (LAMMPS) molecular dynamics simulator.¹⁶

The Li ion distribution in the system was analyzed with the pair correlation function,

$g_{A-B}(r)$:

$$g_{A-B}(r) = \left(\frac{n_B}{4\pi r^2 dr} \right) / \left(\frac{N_B}{V} \right) \quad (2)$$

, where, n_B is the number of B particles located at a distance r in a shell with a thickness dr from the A particles; N_B is the number of B particles in the system, and V is the total volume of the system, respectively.

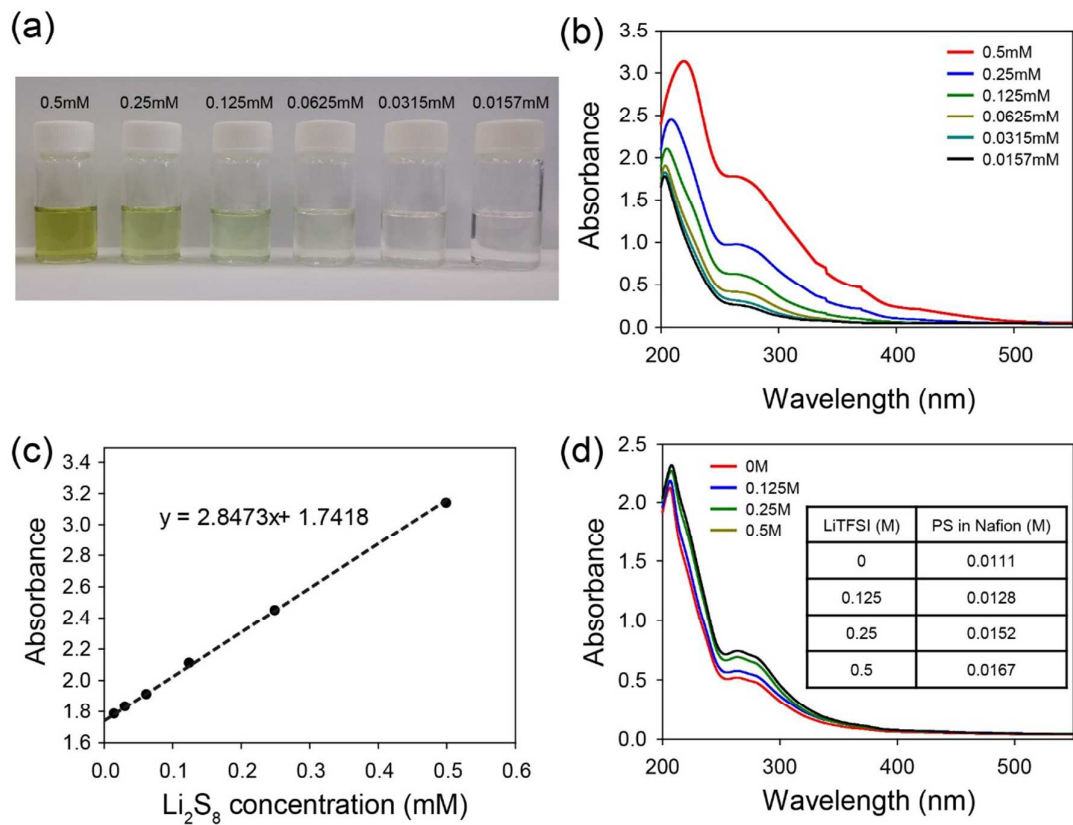


Figure S7. (a) Photo images and (b) UV spectra of the Li_2S_8 solutions in 50S/50D with different Li_2S_8 concentrations. (c) Plot of the absorbance at a wave length of 230 nm as a function of the Li_2S_8 concentration. (d) UV spectra of the extract in 50/50 sulfolane/diglyme mixture from the SPSIC equilibrated with 0.1 M Li_2S_8 and different LiTFSI concentrations in the sulfolane/diglyme mixture (50/50 in volume).

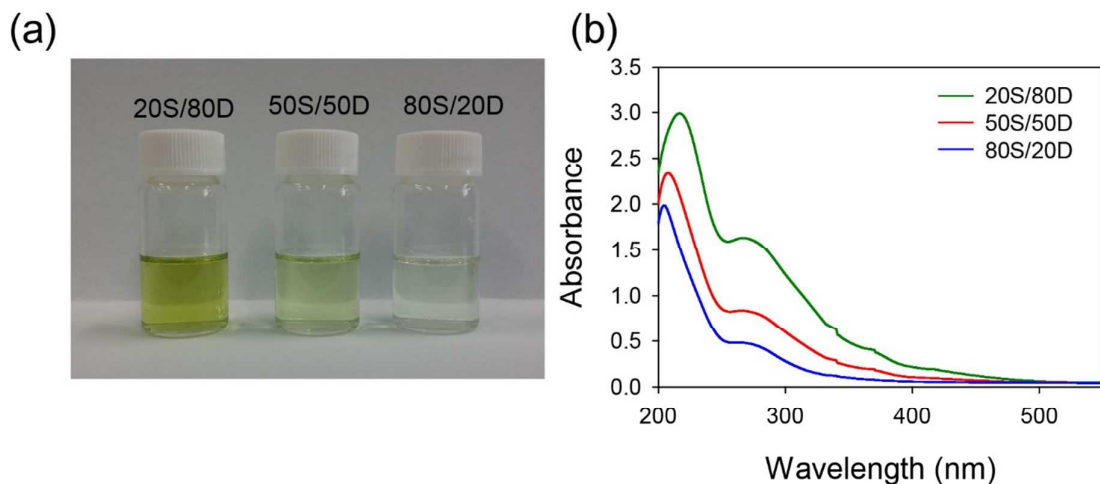


Figure S8. (a) The photo image of the saturated Li_2S_8 solutions in 20S/80D, 50S/50D, and 80S/20D. The saturated solutions were obtained from the supernatants of 1.5 M Li_2S_8 solutions in 20S/80D, 50S/50D, and 80S/20D. (b) UV spectra of the diluted Li_2S_8 solutions. For UV measurement, the saturated solutions were diluted 6000 times with DME.

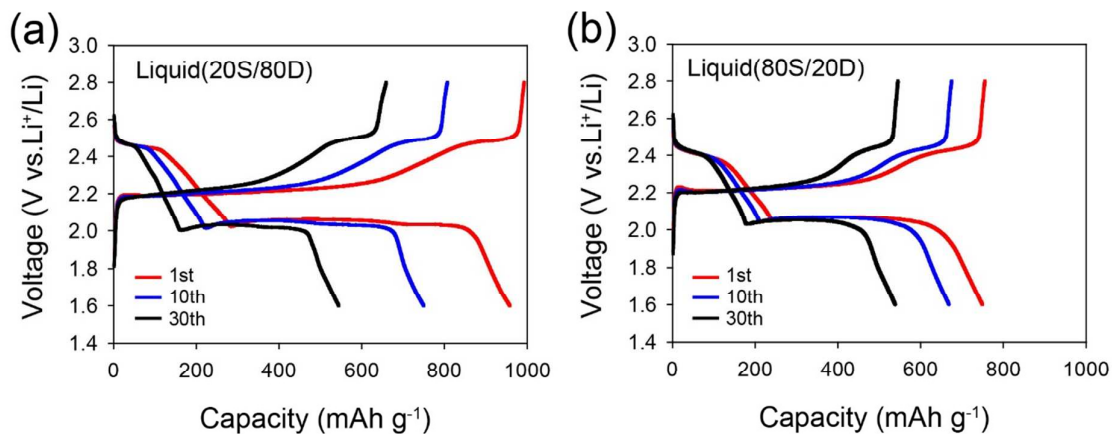


Figure S9. Galvanostatic charge/discharge voltage profiles for the liquid electrolyte cells based on 1 M LiTFSI (a) 20S/80D and (b) 80S/20D electrolyte.

References

- (1) Song, J.; Choo, M. J.; Noh, H.; Park, J. K.; Kim, H. T. Perfluorinated ionomer-enveloped sulfur cathodes for lithium-sulfur batteries. *ChemSusChem* **2014**, *7*, 3341-6.
- (2) Song, J.; Noh, H.; Lee, H.; Lee, J.-N.; Lee, D. J.; Lee, Y.; Kim, C. H.; Lee, Y. M.; Park, J.-K.; Kim, H.-T. Polysulfide rejection layer from alpha-lipoic acid for high performance lithium-sulfur battery. *J. Mater. Chem. A* **2015**, *3*, 323-330.
- (3) Bauer, I.; Thieme, S.; Brückner, J.; Althues, H.; Kaskel, S. Reduced polysulfide shuttle in lithium-sulfur batteries using Nafion-based separators. *J. Power Sources* **2014**, *251*, 417-422.
- (4) Ma, L.; Nath, P.; Tu, Z.; Tikekar, M.; Archer, L. A. Highly Conductive, Sulfonated, UV-Cross-Linked Separators for Li-S Batteries. *Chem. Mater.* **2016**, *28*, 5147-5154.
- (5) Jang, S. S.; Molinero, V.; Cagin, T.; Goddard, W. A. Nanophase-segregation and transport in Nafion 117 from molecular dynamics simulations: effect of monomeric sequence. *J. Phys. Chem. B* **2004**, *108*, 3149-3157.
- (6) Brunello, G.; Lee, S. G.; Jang, S. S.; Qi, Y. A molecular dynamics simulation study of hydrated sulfonated poly (ether ether ketone) for application to polymer electrolyte membrane fuel cells: Effect of water content. *J. Renewable and Sustainable Energy* **2009**, *1*, 033101.
- (7) Lee, S. G.; Brunello, G. F.; Jang, S. S.; Bucknall, D. G. Molecular dynamics simulation study of P (VP-co-HEMA) hydrogels: Effect of water content on equilibrium structures and mechanical properties. *Biomaterials* **2009**, *30*, 6130-6141.
- (8) Lee, S. G.; Brunello, G. F.; Jang, S. S.; Lee, J. H.; Bucknall, D. G. Effect of monomeric sequence on mechanical properties of P (VP-co-HEMA) hydrogels at low hydration. *J. Phys. Chem. B* **2009**, *113*, 6604-6612.

- (9) Mayo, S. L.; Olafson, B. D.; Goddard, W. A. DREIDING: a generic force field for molecular simulations. *J. Phys. Chem.* **1990**, *94*, 8897-8909.
- (10) Jang, S. S.; Goddard, W. A. Structures and transport properties of hydrated water-soluble dendrimer-grafted polymer membranes for application to polymer electrolyte membrane fuel cells: classical molecular dynamics approach. *J. Phys. Chem. C* **2007**, *111*, 2759-2769.
- (11) Jang, S. S.; Lin, S.-T.; Çagin, T.; Molinero, V.; Goddard, W. A. Nanophase segregation and water dynamics in the dendrion diblock copolymer formed from the Frechet polyaryl ethereal dendrimer and linear PTFE. *J. Phys. Chem. B* **2005**, *109*, 10154-10167.
- (12) Brunello, G. F.; Lee, J. H.; Lee, S. G.; Choi, J. I.; Harvey, D.; Jang, S. S. Interactions of Pt nanoparticles with molecular components in polymer electrolyte membrane fuel cells: multi-scale modeling approach. *RSC Advances* **2016**, *6*, 69670-69676.
- (13) Lee, S. G.; Koh, W.; Brunello, G. F.; Choi, J. I.; Bucknall, D. G.; Jang, S. S. Effect of monomeric sequence on transport properties of d-glucose and ascorbic acid in poly (VP-co-HEMA) hydrogels with various water contents: molecular dynamics simulation approach. *Theoretical Chemistry Accounts* **2012**, *131*, 1-16.
- (14) Kumar, N.; Seminario, J. M. Lithium-Ion Model Behavior in an Ethylene Carbonate Electrolyte Using Molecular Dynamics. *J. Phys. Chem. C* **2016**, *120*, 16322-16332.
- (15) Mulliken, R. S. Electronic population analysis on LCAO-MO molecular wave functions. I. *J. Chem. Physics* **1955**, *23*, 1833-1840.
- (16) Plimpton, S. Fast parallel algorithms for short-range molecular dynamics. *J. Comput. Physics* **1995**, *117*, 1-19.